Heisenberg antiferromagnet and the XY model at $T = 0$ in three dimensions

J. Oitmaa,* C.J. Hamer,† and Zheng Weihong‡
School of Physics, The University of New South Wales, Sydney, New South Wales 2052, Australia
(Received 23 March 1994)

The spin-$\frac{1}{2}$ and spin-1 Heisenberg antiferromagnet and XY model are studied at zero temperature on the simple cubic, body-centered-cubic, and (for the XY case only) face-centered cubic lattices. Series expansions around the Ising limit are calculated, for the ground-state energy, staggered magnetization, transverse susceptibility, staggered parallel susceptibility, energy gap and dispersion relation, using a linked-cluster technique. The results are compared with spin-wave perturbation theory, which has been extended to third order for the Heisenberg antiferromagnet, and the agreement is excellent. The finite-size scaling corrections which are calculated from the spin-wave theory are also entirely consistent with the predictions of effective-Langrangian theory.

I. INTRODUCTION

The Heisenberg antiferromagnet on a square lattice has recently attracted much attention,[1] due to its possible connection with high-T_c superconductors. Following work of Singh,[2] we were able to show[3] that results of high accuracy can be obtained for the zero-temperature limit of the model using series expansions about the Ising limit. Their accuracy has only recently been matched, in fact, by the quantum Monte Carlo calculations of Runge.[4] Furthermore, it was shown that spin-wave theory agrees very well with the series results, when carried to higher orders,[3,5] and that the spin-wave theory also gives detailed predictions for the finite-size scaling corrections in the model,[6] which are consistent with universal formulas derived from the effective-Langrangian approach.[7–9] Similar results were also obtained for the quantum XY model at zero temperature on the square lattice.[10]

In view of these results, our purpose in this paper is to apply the same techniques to the three-dimensional versions of these models. There are many real magnetic systems which may be described by these models in three dimensions: See for example the reviews by de Jongh and Miedema[11] and Betts.[12] The lattice coordination number is generally larger in three dimensions than in two, and so the quantum fluctuations are less effective in reducing the long-range order. As a result, spin-wave theory and the series expansions should be even more accurate. These expectations are borne out by our results.

The study of quantum spin systems in three dimensions has a long history.[13] The existence of long-range order in these models on the cubic lattice at low temperatures has been rigorously proven by Dyson, Lieb, and Simon,[14] Kennedy, Lieb, and Shastry,[15] and Kubo and Kishi.[16] The development of spin-wave theory for the Heisenberg antiferromagnet goes back to early work by Anderson,[17] Kubo,[18] Oguchi,[19] and Stinchcombe,[20] among others. Nishimori and Miyake[21] have given a self-consistent spin-wave treatment to second order. Spin-wave theory was previously thought to be unsatisfactory in the case of the XY model,[13] but recently Gomez-Santos and Joannopoulos[22] have shown that, by a difference choice of quantization axis, an accurate theory can be developed. Variational approximations have been used in early work by Marshall[23] and Taketa and Nakamura.[24] Perturbation expansions about the Ising limit have been used by Davis[25] and Parinello and Arai[26] for the Heisenberg model. A related approach, using projection operator techniques, has been developed by Becker, Won, and Fulde[27] and applied to three-dimensional lattices by Kim and Hong.[28] However, long expansions, comparable to those in two dimensions, have not previously been obtained for three-dimensional lattices. A finite-cell calculation has been presented by Oitmaa and Betts,[29] for both the Heisenberg and XY models. Quantum Monte Carlo simulations have been confined to the two-dimensional models, as far as we are aware.

The remainder of the paper is set out as follows. In Sec. II we briefly describe the method of derivation of the series, discuss some technical details, and present results. Series are obtained for the ground-state energy, staggered magnetization, parallel staggered susceptibility, uniform perpendicular susceptibility, and energy gap. In Sec. III we develop spin wave theory to third order for the Heisenberg antiferromagnet on the simple-cubic (sc) and body-centred-cubic (bcc) lattices. Results are obtained for all above quantities as well as for the spin-wave velocity. Finite-size scaling corrections are discussed and compared with the predictions of effective-Lagrangian theory. We have previously given a second-order spin-wave analysis for the XY model on the three dimensional lattices.[30] In Sec. IV we present an analysis of the series and a comparison of the results of both approaches. The agreement is extremely good. Finally in Sec. V we give a summary and conclusions.

II. DERIVATION OF SERIES

We consider the anisotropic Heisenberg antiferromagnet (XXZ model) with Hamiltonian:

$$H = \sum_{\langle lm\rangle}[S_l^z S_m^z + x(S_l^x S_m^x + S_l^y S_m^y)] , \quad (1)$$

where $\langle lm\rangle$ denotes a sum over all nearest-neighbor pairs. The limits $x = 0$ and $x = 1$ correspond to the antiferromagnetic Ising model, and isotropic Heisenberg model respectively. We also consider the anisotropic quantum XY model

$$H = -\sum_{\langle lm\rangle}(S_l^x S_m^x + x S_l^y S_m^y). \quad (2)$$

In each case the Hamiltonian has the form $H = H_0 + xV$ and we seek to derive long perturbation expansions in the anisotropy parameter x, i.e., about the Ising limit.

Our approach uses a cluster expansion method due to Nickel,[31] which has been explained in some detail in one of our earlier papers.[32] We present here a brief summary of the essential ideas.

To obtain the ground-state energy E_0^N for a lattice of N sites one considers a set of clusters $\{\alpha\}$ and writes

$$E_0^N = \sum_\alpha C_\alpha^N \varepsilon_\alpha , \quad (3)$$

where C_0^N is the embedding constant for cluster α and ε_α is the "cumulant energy" of cluster α, as defined below. The ground-state energy for cluster β can also be written

$$E_0^\beta = \sum_\alpha C_\alpha^\beta \varepsilon_\alpha , \quad (4)$$

and this results in an iterative method for obtaining the cumulant energies ε_α via the ground-state energies of a set of clusters of increasing size. The ground-state energies E_0^β are obtained as power series in x through an efficient computerized Rayleigh-Schrödinger perturbation algorithm. The calculation of the energy gap is a little more involved and we refer the reader to Ref. 32 for further details.

What is needed then is the following information.

(i) A list of all clusters up to the order required. For the expansions considered here the clusters are grouped according to the number of sites or vertices. An efficient computer algorithm is used to generate all connected clusters.

TABLE I. The number of clusters generated for each lattice.

	Ground-state energy		Energy gap	
	Order	No. of Clusters	Order	No. of clusters
sc lattice	12	12280	11	5510
bcc lattice	12	49021	11	15295
fcc lattice	9	7215	9	9431

(ii) The embedding constants C_α^N. These are the "strong" or low-temperature lattice constants, in standard terminology, and are enumerated by direct counting or algebraic reduction methods.

(iii) For each cluster α, a list of subclusters and corresponding embedding constants. For the ground state only connected clusters are needed while for the energy gap disconnected clusters, including those with one isolated vertex, are also needed. Table I gives the number of clusters generated for each lattice. Not all of these in fact contribute to the order of the series obtained, the acceptance ratio being of order 50%.

A number of checks with previous work have been made. The list of connected clusters and their embedding constants may be used to define a generating function

$$F(x,b) = \sum_r A_r(b)x^r , \quad (5)$$

where $A_r(b)$ is a polynomial whose coefficients give the number of connected r-site clusters with various numbers of bonds (edges). Sykes and Wilkinson[33] and Sykes[34] have given the A_r's to order 13 for the sc and bcc lattices, respectively. Our data agree completely with these results. The data for connected and disconnected clusters can be used to compute the low-temperature polynomials $L_r(u)$ for the Ising model.[35] The polynomials obtained in this way agree completely with published results for the sc lattice,[35] the bcc lattice,[35,36] and fcc lattice to order 8.[35,36] The polynomial L_9, which is obtained from our data as

$$\begin{aligned} L_9 = {} & 80u^{33} + 438u^{34} + 1776u^{35} + 6976u^{36} + 23898u^{37} + 46567u^{38} + 126346u^{39} \\ & +53220u^{40} - 179270u^{41} - 1353313u^{42} - 6743976u^{43} - 4449786u^{44} - 37125033\tfrac{1}{3}u^{45} \\ & +192574385u^{46} + 452391180u^{47} - 1018385574u^{48} - 4958299828u^{49} + 18998141497u^{50} \\ & -27672861980u^{51} + 20978781848u^{52} - 8269648148u^{53} + 1346898697\tfrac{4}{9}u^{54}, \end{aligned} \quad (6)$$

is, to the best of our knowledge, new.

For the XXZ model, series have been calculated for the ground-state energy per site E_0/N, the energy gap m, the staggered magnetization M^+, the parallel staggered susceptibility $\chi_\parallel^S$, and the uniform perpendicular susceptibility $\chi_\perp$. The staggered perpendicular susceptibility $\chi_\perp^S$ is related to $\chi_\perp$ by the relation $\chi_\perp^S(x) = \chi_\perp(-x)$. The resulting series for the spin-$\frac{1}{2}$ and spin-1 Heisenberg antiferromagnets on the sc and bcc lattices are listed in Tables II and III.

For the XY model on bipartite lattices, such as the sc and bcc lattices, the isotropic antiferromagnetic model

$$H^A = \sum_{\langle lm\rangle}(S_l^x S_m^x + S_l^y S_m^y) , \quad (7)$$

is related to the ferromagnetic one by a simple spin transformation. Hence, there exist the following relations between the isotropic XY ferromagnet (F), antiferromagnet (A), and the model described by Eq. (2):

TABLE II. Series coefficients for the ground-state energy per site E_0/N, the staggered magnetization M^+, staggered parallel susceptibility $\chi_\parallel^S$, and the energy gap m. Coefficients of x^n are listed for both the spin-$\frac{1}{2}$ and spin-1 Heisenberg antiferromagnets.

n	E_0/N	M^+	$\chi_\parallel^S$	m
Spin-$\frac{1}{2}$ XXZ model on the sc lattice				
0	$-3/4$	$1/2$	0	3
2	$-1.500000000000\times10^{-1}$	$-6.000000000000\times10^{-2}$	$4.800000000000\times10^{-2}$	-1.95
4	$5.000000000000\times10^{-4}$	$-4.011111111111\times10^{-3}$	$1.437209876543\times10^{-2}$	$-7.480952380952\times10^{-2}$
6	$-1.565320944488\times10^{-3}$	$-3.724431496528\times10^{-3}$	$1.172820560775\times10^{-2}$	$-2.386949857024\times10^{-1}$
8	$-4.704476286333\times10^{-4}$	$-1.921150493841\times10^{-3}$	$8.712598733252\times10^{-3}$	$-3.884790029204\times10^{-2}$
10	$-2.617515568853\times10^{-4}$	$-1.282583243920\times10^{-3}$	$7.077235096534\times10^{-3}$	$-1.028725932747\times10^{-1}$
12	$-1.500007148263\times10^{-4}$	$-9.023859053626\times10^{-4}$	$5.955040359990\times10^{-3}$	
Spin-1 XXZ model on the sc lattice				
0	-3	1	0	6
2	$-2.727272727273\times10^{-1}$	$-4.958677685950\times10^{-2}$	$1.803155522164\times10^{-2}$	-3.327272727273
4	$-1.656649135988\times10^{-2}$	$-1.072887293023\times10^{-2}$	$9.078996187332\times10^{-3}$	$-6.352818729770\times10^{-1}$
6	$-4.402238091215\times10^{-3}$	$-4.729751792196\times10^{-3}$	$6.071618928288\times10^{-3}$	$-3.345548334284\times10^{-1}$
8	$-1.834625905661\times10^{-3}$	$-2.741948288721\times10^{-3}$	$4.682294372222\times10^{-3}$	$-2.098357436338\times10^{-1}$
10	$-9.267889233149\times10^{-4}$	$-1.779143740889\times10^{-3}$	$3.797492779253\times10^{-3}$	$-1.472426300104\times10^{-1}$
12	$-5.334684310134\times10^{-4}$	$-1.249464211646\times10^{-3}$	$3.196605888446\times10^{-3}$	
Spin-$\frac{1}{2}$ XXZ model on the bcc lattice				
0	-1	$1/2$	0	4
2	$-1.428571428571\times10^{-1}$	$-4.081632653061\times10^{-2}$	$2.332361516035\times10^{-2}$	-2.380952380952
4	$-4.877775285939\times10^{-3}$	$-6.429355947185\times10^{-3}$	$1.006610968929\times10^{-2}$	$-3.196285196285\times10^{-1}$
6	$-1.649666357885\times10^{-3}$	$-3.035412156556\times10^{-3}$	$6.737938708739\times10^{-3}$	$-2.252299684735\times10^{-1}$
8	$-6.929303903362\times10^{-4}$	$-1.773699786862\times10^{-3}$	$5.198354403799\times10^{-3}$	$-1.264167954066\times10^{-1}$
10	$-3.520035082119\times10^{-4}$	$-1.154245309679\times10^{-3}$	$4.216698493871\times10^{-3}$	$-9.455214371223\times10^{-2}$
12	$-2.037541131770\times10^{-4}$	$-8.129275009943\times10^{-4}$	$3.550840789723\times10^{-3}$	
Spin-1 XXZ model on the bcc lattice				
0	-4	1	0	8
2	$-2.666666666667\times10^{-1}$	$-3.555555555556\times10^{-2}$	$9.481481481481\times10^{-3}$	-4.304761904762
4	$-1.991315453384\times10^{-2}$	$-8.848010368105\times10^{-3}$	$5.202442595704\times10^{-3}$	$-9.097495817418\times10^{-1}$
6	$-5.314050576463\times10^{-3}$	$-3.986869676812\times10^{-3}$	$3.579041013496\times10^{-3}$	$-4.596687578938\times10^{-1}$
8	$-2.168020096514\times10^{-3}$	$-2.281649098940\times10^{-3}$	$2.742143507967\times10^{-3}$	$-2.877155097259\times10^{-1}$
10	$-1.093837681014\times10^{-3}$	$-1.480212403691\times10^{-3}$	$2.225922465809\times10^{-3}$	$-2.018710900252\times10^{-1}$

$$E_0(x=1) = E_0(x=-1) = E_0^A = E_0^F \,, \tag{8a}$$
$$M_x(x=1) = M_x(x=-1) = M_x^F = M_x^{A,S} \,, \tag{8b}$$
$$\chi_{xx}(x=1) = \chi_{xx}(x=-1) = \chi_{xx}^F = \chi_{xx}^{A,S}, \tag{8c}$$
$$\chi_{yy}(x=1) = \chi_{yy}^{A,S} = \chi_{yy}^F, \tag{8d}$$
$$\chi_{yy}(x=-1) = \chi_{yy}^A = \chi_{yy}^{F,S}, \tag{8e}$$
$$\chi_{zz}(x=1) = \chi_{zz}^A = \chi_{zz}^F, \tag{8f}$$
$$\chi_{zz}(x=-1) = \chi_{zz}^{A,S} = \chi_{zz}^{F,S}, \tag{8g}$$

where the superscript S denotes the staggered magnetization and susceptibility. The fcc lattice is not a bipartite lattice, and the ground-state energy E_0 and its derivatives are functions of x, rather than functions of x^2 as in the case of bipartite lattices. The resulting series for the spin-$\frac{1}{2}$ XY model on sc, bcc, and fcc lattices are listed in Tables IV and V.

III. THIRD-ORDER SPIN-WAVE RESULTS FOR THE XXZ MODEL

The general third-order spin-wave theory and its application to the square lattice has been discussed in Refs. 5, 6, where the physical quantities are mainly functions of $C_n(x)$ defined by

TABLE III. Series coefficients for the perpendicular susceptibility $\chi_\perp$. Coefficients of x^n are listed for both the spin-$\frac{1}{2}$ and spin-1 Heisenberg antiferromagnets on the sc and bcc lattices.

n	Spin-$\frac{1}{2}$ sc	Spin-1 sc	Spin-$\frac{1}{2}$ bcc	Spin-1 bcc
0	1/6	1/6	1/8	1/8
1	$-1/5$	$-2/11$	$-1/7$	$-2/15$
2	0.2047619047619	0.1827651515152	0.1446428571429	0.1337121212121
3	-0.2089841269841	-0.1855011895818	-0.1475695223144	-0.1353154533844
4	0.2093120630912	0.1857250599719	0.1478680866468	0.1354155330063
5	-0.2110707085205	-0.1867456123021	-0.1489148208821	-0.1360495759429
6	0.2113749749681	0.1868243559399	0.1490393875942	0.1360873635876
7	-0.2122818126498	-0.1873888712210	-0.1496187218766	-0.1364307482710
8	0.2124299805549	0.1874341182247	0.1496933120095	0.1364510018592
9	-0.2130062125841	-0.1877882149073	-0.1500571373779	-0.1366669886154
10	0.2131115958540	0.1878171707705	0.1501053807278	
11	-0.2135065810254	-0.1880607495981	-0.1503559053134	

$$C_n(x) = \frac{2}{N}\sum_k [(1 - x^2\gamma_k^2)^{n/2} - 1], \tag{9}$$

and the structure factor γ_k is defined by

$$\gamma_k = \frac{1}{z}\sum_\rho e^{ik\cdot\rho}. \tag{10}$$

z is the coordination number, and the sum over k denotes a sum over the first Brillouin zone of the sublattice l. For a bulk system, the momentum k is continuous over the first Brillouin zone, but for a finite-lattice system, the momentum k is discrete. For the sc and bcc lattices, the structure factor γ_k, the first Brillouin zone for the bulk system, and the discrete momenta k for a finite-lattice system are the following:

(1) sc lattice:

$$\gamma_k = [\cos(k_x a) + \cos(k_y a) + \cos(k_z a)]/3 \ , \tag{11}$$

momentum k:

$$-\pi/a < k_x, k_y \le \pi/a, \ |k_z| \le \pi/(2a), \quad \text{bulk system},$$

$$k_x(i), k_y(i) = \frac{2\pi i}{aL}, \quad i = 1, 2, \ldots, L,$$

$$k_z(j) = \frac{2\pi j}{aL}, \quad j = 1, 2, \ldots, L/2, \quad \text{finite lattice system.}$$

(2) bcc lattice:

$$\gamma_k = \cos(k_x a/2)\cos(k_y a/2)\cos(k_z a/2) \ , \tag{12}$$

momentum k:

$$-\pi/a < k_x, k_y, k_z \le \pi/a, \quad \text{bulk system},$$

$$k_x(i), k_y(i), k_z(i) = \frac{2\pi i}{aL},$$

$$i = 1, 2, \ldots, L, \quad \text{finite-lattice system},$$

where L and a are the lattice size and the lattice spacing, respectively. For convenience, we set the lattice spacing $a = 1$ from now on. For a bulk system, the asymptotic behavior near $x = 1$ of C_n is given in Ref. 30. We must note that the singularity here is different from that on the square lattice, where the singular terms are of the form $(1 - x^2)^{n/2}$, whereas here the singular terms are of the form $(1 - x^2)^n \ln(1 - x^2)$ (n is a integer). The finite-size corrections to C_i can be calculated in the same way as for the square lattice.[6] The results are the following:

(1) sc lattice:

TABLE IV. Series coefficients for the ground-state energy per site E_0/N, the magnetization M_x, and the parallel susceptibility χ_{xx} of the spin-$\frac{1}{2}$ XY model. Coefficients of x^n are listed.

n	E_0/N	M_x	χ_{xx}
Spin-$\frac{1}{2}$ XY model on the sc lattice			
0	$-3/4$	$1/2$	0
2	$-3.750000000000\times10^{-2}$	$-1.500000000000\times10^{-2}$	$1.200000000000\times10^{-2}$
4	$-2.781250000000\times10^{-3}$	$-3.438194444444\times10^{-3}$	$5.723256172840\times10^{-3}$
6	$-7.641105083510\times10^{-4}$	$-1.575367408278\times10^{-3}$	$3.932928543228\times10^{-3}$
8	$-3.116037629649\times10^{-4}$	$-9.011185812862\times10^{-4}$	$3.001822149165\times10^{-3}$
10	$-1.569872619187\times10^{-4}$	$-5.840152277071\times10^{-4}$	$2.431110482685\times10^{-3}$
12	$-9.016114952890\times10^{-5}$	$-4.099185424317\times10^{-4}$	$2.046130221965\times10^{-3}$
Spin-$\frac{1}{2}$ XY model on the bcc lattice			
0	-1	$1/2$	0
2	$-3.571428571429\times10^{-2}$	$-1.020408163265\times10^{-2}$	$5.830903790087\times10^{-3}$
4	$-3.334197690065\times10^{-3}$	$-2.890218493055\times10^{-3}$	$3.357080496772\times10^{-3}$
6	$-9.009318847504\times10^{-4}$	$-1.316221737101\times10^{-3}$	$2.317905365556\times10^{-3}$
8	$-3.672948080736\times10^{-4}$	$-7.540401362783\times10^{-4}$	$1.776563284100\times10^{-3}$
10	$-1.852091587882\times10^{-4}$	$-4.895797329177\times10^{-4}$	$1.443527472221\times10^{-3}$
12	$-1.064041460129\times10^{-4}$	$-3.439572927014\times10^{-4}$	$1.217306755892\times10^{-3}$
Spin-$\frac{1}{2}$ XY model on the fcc lattice			
0	$-3/2$	$1/2$	0
1	0	0	0
2	$-3.409090909091\times10^{-2}$	$-6.198347107438\times10^{-3}$	$2.253944402705\times10^{-3}$
3	$-6.198347107438\times10^{-3}$	$-2.253944402705\times10^{-3}$	$1.229424219657\times10^{-3}$
4	$-2.475737616016\times10^{-3}$	$-1.388229359974\times10^{-3}$	$1.039956403788\times10^{-3}$
5	$-1.184735853462\times10^{-3}$	$-8.912659135055\times10^{-4}$	$8.397087738470\times10^{-4}$
6	$-6.643312716138\times10^{-4}$	$-6.283570849856\times10^{-4}$	$7.148069660409\times10^{-4}$
7	$-4.094622435794\times10^{-4}$	$-4.661098853272\times10^{-4}$	$6.204928498120\times10^{-4}$
8	$-2.706300376371\times10^{-4}$	$-3.601275380037\times10^{-4}$	$5.490230234957\times10^{-4}$
9	$-1.883309173349\times10^{-4}$	$-2.867757000281\times10^{-4}$	$4.924784303546\times10^{-4}$

$$C_3(1) = -0.220369512500 + 3.932/L^6 + O(L^{-7}) , \quad (13a)$$

$$C_1(1) = -0.0971580039513 - 1.934209/L^4 + O(L^{-5}) , \quad (13b)$$

$$C_{-1}(1) = 0.156715415334 - 1.5642841/L^2 + O(L^{-3}) . \quad (13c)$$

(2) bcc lattice:

$$C_3(1) = -0.164974389703 + 1.2769393/L^6 + O(L^{-7}) , \quad (14a)$$

$$C_1(1) = -0.0730376707635 - 0.83753691/L^4 + O(L^{-5}) , \quad (14b)$$

$$C_{-1}(1) = 0.118636387164 - 0.903139838/L^2 + O(L^{-3}) . \quad (14c)$$

A. Ground-state energy

As discussed in Ref. 5, there are two perturbation terms $\Delta E_a^{(-1)}$ and $\Delta E_b^{(-1)}$ contributing to the third-order spin-wave results for the ground-state energy, and at the isotropic limit $x = 1$,

$$\Delta E_a^{(-1)} = 0 , \quad (15)$$

while $\Delta E_b^{(-1)}$ is a nine-dimensional integral over the first Brillouin zone of the sublattice l. It can be computed numerically in the follow way: We first evaluate its value for finite lattices, and then extrapolate the results to the infinite lattice:

TABLE V. Series coefficients for the transverse susceptibility χ_{yy}, χ_{zz}, and the energy gap m of the spin-$\frac{1}{2}$ XY model. Coefficients of x^n are listed.

n	χ_{yy}	χ_{zz}	m
Spin-$\frac{1}{2}$ XY model on the sc lattice			
0	1/6	1/6	3
1	$1.833333333333\times10^{-1}$	$-1.666666666667\times10^{-2}$	-1.5
2	$1.845238095238\times10^{-1}$	$1.190476190476\times10^{-3}$	$-4.875000000000\times10^{-1}$
3	$1.873815192744\times10^{-1}$	$-6.978458049887\times10^{-4}$	$-1.359375000000\times10^{-1}$
4	$1.876285109968\times10^{-1}$	$5.022852635523\times10^{-5}$	$-1.249490327381\times10^{-1}$
5	$1.888562013916\times10^{-1}$	$-1.320188413512\times10^{-4}$	$-6.784615593850\times10^{-2}$
6	$1.889751210970\times10^{-1}$	$9.887227440714\times10^{-7}$	$-6.115068171845\times10^{-2}$
7	$1.896483343876\times10^{-1}$	$-4.469817979089\times10^{-5}$	$-4.146406000229\times10^{-2}$
8	$1.897187379037\times10^{-1}$	$-3.315611370521\times10^{-6}$	$-3.804881048189\times10^{-2}$
9	$1.901446928063\times10^{-1}$	$-2.000372946766\times10^{-5}$	$-2.859252703493\times10^{-2}$
10	$1.901917971750\times10^{-1}$	$-2.979158322603\times10^{-6}$	$-2.658763363254\times10^{-2}$
11	$1.904864449354\times10^{-1}$	$-1.060246590636\times10^{-5}$	
Spin-$\frac{1}{2}$ XY model on the bcc lattice			
0	1/8	1/8	4
1	15/112	$-1/112$	-2
2	$1.343750000000\times10^{-1}$	$4.464285714286\times10^{-4}$	$-5.952380952381\times10^{-1}$
3	$1.362220193709\times10^{-1}$	$-3.993152893025\times10^{-4}$	$-2.182539682540\times10^{-1}$
4	$1.363488832957\times10^{-1}$	$2.436475105581\times10^{-5}$	$-1.617946207232\times10^{-1}$
5	$1.371121252412\times10^{-1}$	$-8.208795576602\times10^{-5}$	$-9.604697554830\times10^{-2}$
6	$1.371688102888\times10^{-1}$	$1.363244106281\times10^{-7}$	$-8.165041651170\times10^{-2}$
7	$1.375882716948\times10^{-1}$	$-2.857220803419\times10^{-5}$	$-5.764716973423\times10^{-2}$
8	$1.376213752550\times10^{-1}$	$-1.859653069981\times10^{-6}$	$-5.108953815332\times10^{-2}$
9	$1.378873939349\times10^{-1}$	$-1.308177910311\times10^{-5}$	$-3.951012871692\times10^{-2}$
10	$1.379094065898\times10^{-1}$	$-1.618780389665\times10^{-6}$	$-3.578620551813\times10^{-2}$
11	$1.380935429306\times10^{-1}$	$-7.047955217065\times10^{-6}$	
Spin-$\frac{1}{2}$ XY model on the fcc lattice			
0	1/12	1/12	6
1	23/264	$-1/264$	-3
2	$8.836733815427\times10^{-2}$	$-1.312844352617\times10^{-4}$	$-8.681818181818\times10^{-1}$
3	$8.900716098023\times10^{-2}$	$-1.073920486615\times10^{-4}$	$-3.550000000000\times10^{-1}$
4	$8.939819341080\times10^{-2}$	$-4.207313931352\times10^{-5}$	$-2.265922408057\times10^{-1}$
5	$8.966174682517\times10^{-2}$	$-2.396277185827\times10^{-5}$	$-1.553594338314\times10^{-1}$
6	$8.985190255424\times10^{-2}$	$-1.440419034214\times10^{-5}$	$-1.164133745557\times10^{-1}$
7	$8.999599726482\times10^{-2}$	$-9.435544252908\times10^{-6}$	$-9.120044923369\times10^{-2}$
8	$9.010912739846\times10^{-2}$	$-6.512212791619\times10^{-6}$	$-7.763085907377\times10^{-2}$

$$\Delta E_b^{(-1)}/N = \begin{cases} 0.0001596(4)/S, & \text{sc lattice,} \\ 0.00008796(6)/S, & \text{bcc lattice.} \end{cases} \quad (16)$$

Via MATHEMATICA, we can compute a series expansion of $\Delta E_b^{(-1)}$ in x up to order x^{20} for the sc lattice, and up to order x^{24} for the bcc lattice. Extrapolating this series using integrated Dlog Padé approximants,[37] one can obtain an estimate near the isotropic limit $x = 1$:

$$\Delta E_b^{(-1)}/N = \begin{cases} 0.00016(4)/S + 0.0009(3)(1-x^2)/S + \cdots, & \text{sc lattice,} \\ 0.0000888(10)/S + 0.00059(4)(1-x^2)/S + \cdots, & \text{bcc lattice.} \end{cases} \quad (17)$$

The extrapolation of the full series for E_0/N gives

$$E_0/N = \begin{cases} -0.90246(5) + 0.162(1)(1-x^2) + \cdots, & S=\frac{1}{2}, \text{ sc lattice,} \\ -3.2983(2) + 0.350(2)(1-x^2) + \cdots, & S=1, \text{ sc lattice,} \\ -1.15121(3) + 0.1695(10)(1-x^2) + \cdots, & S=\frac{1}{2}, \text{ bcc lattice,} \\ -4.29739(2) + 0.359(2)(1-x^2) + \cdots, & S=1, \text{ bcc lattice.} \end{cases} \quad (18)$$

By comparing the above results, we can conclude that the asymptotic behavior of the bulk ground-state energy per site for the sc and bcc lattices is

$$e_\infty = \lim_{N\to\infty} E_0/N = -3S^2 - 0.291474011829S - 0.00707975829764 + 0.0001596(4)/S$$
$$+(1-x^2)[0.380811S - 0.0298393606 + 0.0009(3)/S] + \cdots, \quad \text{sc lattice,} \quad (19a)$$
$$e_\infty = \lim_{N\to\infty} E_0/N = -4S^2 - 0.292151S - 0.0053345 + 0.00008796(6)/S$$
$$+[0.38335S - 0.022739 + 0.00059(4)/S](1-x^2) + \cdots, \quad \text{bcc lattice.} \quad (19b)$$

The finite-lattice corrections to the isotropic system are

$$E_0/N - e_\infty = -(5.802627S + 0.2818858)/L^4 + \cdots, \quad \text{sc lattice,} \quad (20a)$$
$$E_0/N - e_\infty = -(3.3501476S + 0.12234349)/L^4 + \cdots, \quad \text{bcc lattice.} \quad (20b)$$

B. Staggered magnetization and parallel staggered susceptibility

Referring again to Ref. 5, near the isotropic limit $x = 1$, we have (we take this opportunity to correct a typographical error in Eq. (2.29) of Ref. 5: the correct formula should be $\Delta M_a^{(-2)} = -(16x^4S^2)^{-1}(1-x^2)(C_{-1}-C_1)\{(1-x^2)[3C_{-5}(C_{-1}-C_1) + 4C_{-1}^2 - 9C_{-1}C_{-3} + 2C_{-3}^2 + 3C_{-3}C_1] + 2C_1(C_{-3}-C_{-1})\}$)

$$\Delta M_a^{(-2)} = \begin{cases} -0.00081162972(1-x^2)\ln(1-x^2)/S^2 + \cdots, & \text{sc lattice,} \\ -0.00035460962(1-x^2)\ln(1-x^2)/S^2 + \cdots, & \text{bcc lattice,} \end{cases} \quad (21)$$

$$S^3\Delta\chi_a^{(-3)} = \begin{cases} -0.0000517687968\ln(1-x^2) + 0.000131881344 + \cdots, & \text{sc lattice,} \\ -0.0000168905622\ln(1-x^2) + 0.000029372845 + \cdots, & \text{bcc lattice.} \end{cases} \quad (22)$$

$\Delta M_b^{(-2)}$ is again a nine-dimensional integral, which upon numerical integration is

$$\Delta M_b^{(-2)} = \begin{cases} 0.000270(2)/S^2, & \text{sc lattice,} \\ 0.0001147(15)/S^2, & \text{bcc lattice.} \end{cases} \quad (23)$$

Series expansions were also carried out for $\Delta M_b^{(-2)}$ and $\Delta\chi_b^{(-3)}$ to order x^{20} on the sc lattice and order x^{36} on the bcc lattice for $\Delta M_b^{(-2)}$, and to order x^{12} on the sc lattice and x^{16} on the bcc lattice for $\Delta\chi_b^{(-3)}$. Extrapolation to the isotropic limit gives

$$S^2\Delta M_b^{(-2)} = \begin{cases} 0.00031(8) - 0.0013(3)(1-x^2)\ln(1-x^2) + \cdots, & \text{sc lattice,} \\ 0.000119(4) - 0.00048(5)(1-x^2)\ln(1-x^2) + \cdots, & \text{bcc lattice,} \end{cases} \quad (24)$$

$$S^3\Delta\chi_b^{(-3)} = \begin{cases} 0.00025(8)\ln(1-x^2) + \cdots, & \text{sc lattice,} \\ 0.00008(3)\ln(1-x^2) - 0.00019(6) + \cdots, & \text{bcc lattice.} \end{cases} \quad (25)$$

The extrapolation of the full series for M^+ and $\chi_\parallel^S$ gives

$$M^+ = \begin{cases} 0.4232(5) - 0.0398(4)(1-x^2)\ln(1-x^2) + \cdots, & S=\frac{1}{2}, \text{ sc lattice,} \\ 0.923(1) - 0.0507(4)(1-x^2)\ln(1-x^2) + \cdots, & S=1, \text{ sc lattice,} \\ 0.4416(6) - 0.0345(4)(1-x^2)\ln(1-x^2) + \cdots, & S=\frac{1}{2}, \text{ bcc lattice,} \\ 0.9413(4) - 0.0418(4)(1-x^2)\ln(1-x^2) + \cdots, & S=1, \text{ bcc lattice,} \end{cases} \tag{26}$$

$$\chi_\parallel^S = \begin{cases} -0.0381(1)\ln(1-x^2) - 0.008(2) + \cdots, & S=\frac{1}{2}, \text{ sc lattice,} \\ -0.019(1)\ln(1-x^2) - 0.011(2) + \cdots, & S=1, \text{ sc lattice,} \\ -0.0226(10)\ln(1-x^2) - 0.008(2) + \cdots, & S=\frac{1}{2}, \text{ bcc lattice,} \\ -0.011(1)\ln(1-x^2) - 0.007(2) + \cdots, & S=1, \text{ bcc lattice.} \end{cases} \tag{27}$$

So we conclude that for the bulk sc and bcc lattices near $x = 1$,

$$\begin{aligned} M^+ &= S - 0.078357708 + 0.000270(2)/S^2 \\ &\quad +[-0.065810 + 0.016707/S - 0.0018(3)/S^2](1-x^2)\ln(1-x^2) + \cdots, \quad \text{sc lattice,} && \text{(28a)} \\ M^+ &= S - 0.059318194 + 0.0001147(15)/S^2 \\ &\quad +[-0.0506606 + 0.00971032/S - 0.00083(5)/S^2](1-x^2)\ln(1-x^2) + \cdots, \text{ bcc lattice,} && \text{(28b)} \\ \chi_\parallel^S &= [-0.0219367/S + 0.00106566/S^2 + 0.00019(4)/S^3]\ln(1-x^2) \\ &\quad -0.0143905/S + 0.00626822/S^2 - 0.0005(3)/S^3 + \cdots, \quad \text{sc lattice,} && \text{(28c)} \\ \chi_\parallel^S &= [-0.012665148/S + 0.000462516/S^2 + 0.00006(3)/S^3]\ln(1-x^2) \\ &\quad -0.0086209/S + 0.0027424/S^2 - 0.00016(6)/S^3 + \cdots, \quad \text{bcc lattice.} && \text{(28d)} \end{aligned}$$

The finite-lattice correction to the staggered magnetization of the isotropic model is

$$\begin{aligned} M_N^+ - M_\infty^+ &= (0.782142 + 0 \times S^{-1})/L^2 + \cdots, \quad \text{sc lattice,} && \text{(29a)} \\ M_N^+ - M_\infty^+ &= (0.45156992 + 0 \times S^{-1})/L^2 + \cdots, \quad \text{bcc lattice.} && \text{(29b)} \end{aligned}$$

C. Energy gap

Here there are five perturbation terms contributing to the energy gap at third order, and three of them can be calculated analytically:

$$S(1-x^2)^{-1/2}(\Delta m_a^{(-1)} + \Delta m_d^{(-1)} + \Delta m_e^{(-1)}) = \begin{cases} -0.048338779 + 0.05012226(1-x^2)\ln(1-x^2), & \text{sc lattice,} \\ -0.036738944 + 0.03884128(1-x^2)\ln(1-x^2), & \text{bcc lattice.} \end{cases} \tag{30}$$

The remaining two can be evaluated by series expansion, the extrapolation to the limit $x = 1$ being

$$S(1-x^2)^{-1/2}(\Delta m_b^{(-1)} + \Delta m_c^{(-1)}) = \begin{cases} 0.046(3) + 0.070(1)(1-x^2)\ln(1-x^2) + \cdots, & \text{sc lattice,} \\ 0.0350(8) + 0.055(2)(1-x^2)\ln(1-x^2) + \cdots, & \text{bcc lattice.} \end{cases} \tag{31}$$

The extrapolation of the full series for the energy gap m gives

$$(1-x^2)^{-1/2}m = \begin{cases} 2.530(2) - 0.11(2)(1-x^2)\ln(1-x^2) + \cdots, & S=\frac{1}{2}, \text{ sc lattice,} \\ 5.534(6) - 0.25(2)(1-x^2)\ln(1-x^2) + \cdots, & S=1, \text{ sc lattice,} \\ 3.525(4) - 0.215(5)(1-x^2)\ln(1-x^2) + \cdots, & S=\frac{1}{2}, \text{ bcc lattice,} \\ 7.526(2) - 0.312(6)(1-x^2)\ln(1-x^2) + \cdots, & S=1, \text{ bcc lattice.} \end{cases} \tag{32}$$

The results of numerical integration are

$$-(2S/z)(1-x^2)^{-1/2}(\Delta m_b^{(-1)} + \Delta m_c^{(-1)}) = \begin{cases} -0.0156788(2), & \text{sc lattice,} \\ -0.0089964(5), & \text{bcc lattice.} \end{cases} \tag{33}$$

Therefore, the results are summarized as

$$(1-x^2)^{-1/2}m = 6S - 0.4701462 - 0.0013024(6)/S + [-0.3948602 + 0.13(2)/S](1-x^2)\ln(1-x^2) + \cdots, \quad \text{sc lattice,} \tag{34a}$$

$$(1-x^2)^{-1/2}m = 8S - 0.474545 - 0.000753(2)/S + [-0.405285 + 0.094(4)/S](1-x^2)\ln(1-x^2) + \cdots, \quad \text{bcc lattice.} \tag{34b}$$

D. Perpendicular susceptibility

Using the Dyson-Maleev formalism, the third-order uniform perpendicular susceptibility is found to be [note that we take this opportunity to correct an error in Ref. 5; the contribution from Fig. 3(a) there should only involve the *unperturbed* energy of the intermediate state, so that the term $m^{(-1)}$ should be dropped from Eq. (2.60), and the correct results for the uniform perpendicular susceptibility $\chi_\perp$ and staggered perpendicular susceptibility $\chi_\perp^S$ for the square lattice are $\chi_\perp = 0.125 - 0.03444695942S^{-1} + 0.00204006(7)S^{-2} + O(S^{-3})$, $(1-x)\chi_\perp^S = 0.25 + 0.06889391884S^{-1} + 0.013546(10)S^{-2} + O(S^{-3})$]

$$\chi_\perp = \chi_\perp^{(0)} + \chi_\perp^{(-1)} + \chi_\perp^{(-2)} + O(S^{-3}), \tag{35}$$

with

$$\chi_\perp^{(0)} = \frac{1}{z(1+x)}, \tag{36a}$$

$$\chi_\perp^{(-1)} = \frac{C_1 - C_{-1}}{2zSx(1+x)}, \tag{36b}$$

$$\chi_\perp^{(-2)} = [(1-x)(1+2x)C_{-1}^2 - (1-x^2)(C_{-1}-C_1)C_{-3} - (1+2x-2x^2)C_{-1}C_1 + C_1^2 x][4S^2 z x^3(1+x)]^{-1} + \chi_g^{(-2)} + \chi_i^{(-2)}, \tag{36c}$$

where $\chi_g^{(-2)} + \chi_i^{(-2)}$ is a six-dimensional integral, which can be carried out by series expansion in x via MATHEMATICA up to order x^{24} for the sc lattice, and up to order x^{30} for the bcc lattice. The extrapolation of this series gives

$$2zS^2(1+x)(\chi_g^{(-2)} + \chi_i^{(-2)}) = \begin{cases} 0.00088(2) - 0.0008(3)(1-x)\ln(1-x) + \cdots, & x=1, \text{ sc lattice,} \\ -0.0315(5) - 0.0858(5)(1-x)\ln(1-x) + \cdots, & x=-1, \text{ sc lattice,} \\ 0.00038(1) - 0.00050(5)(1-x)\ln(1-x) + \cdots, & x=1, \text{ bcc lattice,} \\ -0.01813(10) - 0.050(4)(1-x)\ln(1-x) + \cdots, & x=-1, \text{ bcc lattice.} \end{cases} \tag{37}$$

Analysis of the full series gives

$$\chi_\perp = \begin{cases} 0.06445(10) - 0.075(5)(1-x)\ln(1-x) + \cdots, & S=\tfrac{1}{2}, \text{ sc lattice,} \\ 0.073305(5) - 0.0075085(5)(1-x)\ln(1-x) + \cdots, & S=1, \text{ sc lattice,} \\ 0.051448(5) - 0.0066(2)(1-x)\ln(1-x) + \cdots, & S=\tfrac{1}{2}, \text{ bcc lattice,} \\ 0.056744(1) - 0.004842(5)(1-x)\ln(1-x) + \cdots, & S=1, \text{ bcc lattice,} \end{cases} \tag{38}$$

$$(1-x)\chi_\perp^S = \begin{cases} 0.2155(1) + 0.032(3)(1-x)\ln(1-x) + \cdots, & S=\tfrac{1}{2}, \text{ sc lattice,} \\ 0.18944(10) + 0.01912(10)(1-x)\ln(1-x) + \cdots, & S=1, \text{ sc lattice,} \\ 0.15175(1) + 0.0218(10)(1-x)\ln(1-x) + \cdots, & S=\tfrac{1}{2}, \text{ bcc lattice,} \\ 0.13767(1) + 0.0116(4)(1-x)\ln(1-x) + \cdots, & S=1, \text{ bcc lattice.} \end{cases} \tag{39}$$

The results of numerical integration are

$$4zS^2(1+x)(\chi_g^{(-2)} + \chi_i^{(-2)}) = \begin{cases} 0.001736(8), & x=1, \text{ sc lattice,} \\ 0.0007533(3), & x=1, \text{ bcc lattice.} \end{cases} \tag{40}$$

Therefore, the conclusions for the uniform perpendicular susceptibility $\chi_\perp$ and staggered perpendicular susceptibility $\chi_\perp^S$ near the limit $x \to 1$ are

$$\chi_\perp = \begin{cases} 1/12 - 0.0105780585/S + 0.000550005(20)/S^2 \\ \quad +[-0.0109683399/S + 0.00345(5)/S^2](1-x)\ln(1-x) + \cdots, \text{ sc lattice,} \\ \\ 1/16 - 0.005989814/S + 0.00023051(1)/S^2 \\ \quad +[-0.00633257/S + 0.00145(5)/S^2](1-x)\ln(1-x) + \cdots, \quad \text{bcc lattice,} \end{cases} \tag{41}$$

$$(1-x)\chi_\perp^S = \begin{cases} 1/6 + 0.021156117/S + 0.00164(5)/S^2 \\ \quad +[0.02193667974/S - 0.0027(1)/S^2](1-x)\ln(1-x) + \cdots, \text{ sc lattice,} \\ \\ 1/8 + 0.0119796/S + 0.00072(2)/S^2 \\ \quad +[0.01266514/S - 0.0011(3)/S^2](1-x)\ln(1-x) + \cdots, \quad \text{bcc lattice.} \end{cases} \tag{42}$$

E. Spin-wave velocity

The spin-wave velocity can be calculated as usual from the dispersion relation involving the spin-wave energy $m(k)$ of a single-boson state with momentum k. Here we only consider the isotropic case ($x = 1$):

$$m(k) = m^{(1)}(k) + m^{(0)}(k) + m^{(-1)}(k) + O(S^{-2}) , \tag{43}$$

where

$$m^{(1)}(k) = zS(1-\gamma_k^2)^{1/2} , \tag{44a}$$

$$m^{(0)}(k) = -\frac{z}{2}(1-\gamma_k^2)^{1/2}C_1, \tag{44b}$$

$$m^{(-1)}(k) = -\frac{z}{2S}(1-\gamma_k^2)^{1/2}m_{bc}(k), \tag{44c}$$

and $m_{bc}(k)$ is a six-dimensional integral defined in Ref. 6, which can be carried out in the same way as for the square lattice. Figure 1 shows the dispersion relation along the line $k_x = k_y = k_z$ for the sc and bcc lattices. In the limit $k \to 0$, we get

$$m_{bc}(0) = \begin{cases} -0.00253(4), & \text{sc lattice,} \\ -0.00154(2), & \text{bcc lattice.} \end{cases} \tag{45}$$

Therefore, the energy gap of the isotropic Heisenberg antiferromagnet at the small k limit is

$$m(k) = \begin{cases} 2\sqrt{3}S\left[1 + \frac{0.097158004}{2S} + \frac{0.00506(8)}{(2S)^2} + O(S^{-3})\right]k \ , & \text{sc lattice,} \\ \\ 4S\left[1 + \frac{0.073037671}{2S} + \frac{0.00308(4)}{(2S)^2} + O(S^{-3})\right]k \ , & \text{bcc lattice.} \end{cases} \tag{46}$$

and the spin-wave velocity is

$$v = \begin{cases} 2\sqrt{3}S\left[1 + \frac{0.097158004}{2S} + \frac{0.00506(8)}{(2S)^2} + O(S^{-3})\right] \ , & \text{sc lattice,} \\ \\ 4S\left[1 + \frac{0.073037671}{2S} + \frac{0.00308(4)}{(2S)^2} + O(S^{-3})\right] \ , & \text{bcc lattice.} \end{cases} \tag{47}$$

F. Finite-size scaling

The finite-size scaling behavior of the isotropic Heisenberg antiferromagnet has been predicted by Neuberger and Ziman[7] and Fisher,[8] and has been formulated as a systematic large volume expansion by Hasenfratz and Niedermayer.[9] These predictions are based on general arguments that the large distance behavior will be dominated by massless Goldstone bosons, which are precisely the spin waves or magnons, and result from spontaneous breakdown of the O(3) symmetry of the system. A simple effective Lagrangian can be written down for the Goldstone modes, which at leading order involves just three unknown parameters, which can be taken as the spin-wave velocity v, the helicity modulus or spin-wave stiffness ρ_s, and the staggered magnetization $\Sigma \equiv M^+$. On this basis, universal formulas can be derived for the finite-size scaling corrections, which are compared with our spin-wave results below.

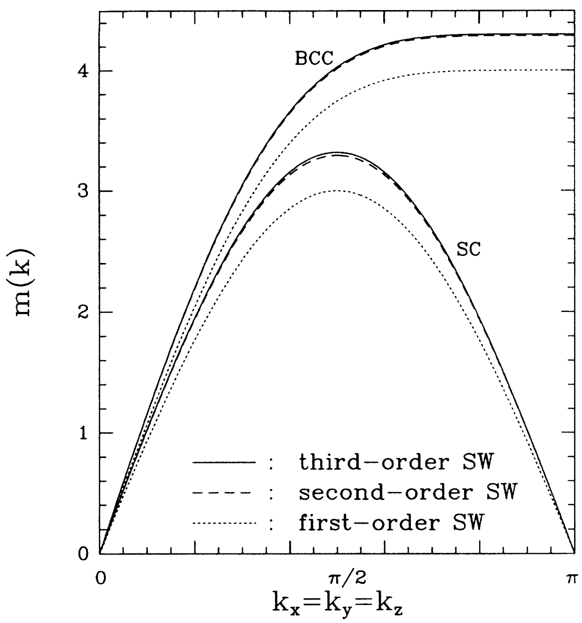

FIG. 1. The spin-wave energy $m(k)$ as a function of momentum k_x along a line $k_x = k_y = k_z$ for the sc and bcc lattices. The three curves shown are the first-, second-, and third-order spin-wave predictions corresponding to short-dashed and solid lines, respectively.

1. Ground-state energy

The predicted finite-size correction to the ground-state energy per site is

$$\frac{E_0}{N} - e_\infty = -\frac{\beta v}{L^{D+1}} + O(L^{-2D}) \ , \tag{48}$$

in D space dimensions, where β is a calculable shape factor appropriate to the particular lattice. According to the notation of Hasenfratz and Leutwyler[38] for a hypercubic lattice

$$\begin{aligned}\beta &= \alpha^{(D)}_{-\frac{1}{2}}(1) + 2 - \frac{2}{D+1} \\ &= 1.675074, \qquad \text{sc lattice.}\end{aligned} \tag{49}$$

Equations (20) and (47) are in precise agreement with the prediction (48) up to the order calculated, with the shape factor β given by (49) for the sc lattice, and $\beta = 0.83753690$ for the bcc lattice. Note that β for the bcc lattice is half that for the sc lattice, probably because the primitive unit cell for the bcc lattice contains two sites but the primitive unit cell for the sc lattice contains only one site (here we take the size of the primitive unit cell to be one lattice unit).

2. Energy gap

The predicted finite-lattice energy gap at zero momentum is

$$m_N(k=1) = \frac{1}{\chi_\perp L^D} + O(L^{1-2D}) \ . \tag{50}$$

The leading-order spin-wave result for this quantity was obtained in a previous paper:[6]

$$m_N(k=1) = \frac{2z}{L^D} + \cdots , \tag{51}$$

where z in the lattice coordination number. Equations (50) and (51) are consistent to leading order.

3. Staggered magnetization

Neuberger and Ziman[7] have discussed the finite-lattice corrections to the staggered magnetization predicted by the effective Lagrangian theory for the square lattice. A generalization which includes their result is

$$M^+_N - M^+_\infty = \frac{\Sigma v \gamma}{\rho_s L^{D-1}} + \cdots \ , \tag{52}$$

where γ is another calculable shape factor. This result must be interpreted with some care. Strictly speaking, there is no spontaneous symmetry breaking on a finite lattice at zero field, and the staggered magnetization is zero. Equation (52) describes the value obtained either at a finite but very small field, or else perhaps by a measure of the mean-square magnetization. In the notation of Hasenfratz and Leutwyler,[38] for a hypercubic lattice

$$\begin{aligned}\gamma &= \frac{1}{4\pi}\left[2 + \frac{2}{D-1} - \alpha^{(D)}_{+\frac{1}{2}}(1)\right] \\ &= \begin{cases} 0.3103732, & \text{square lattice,} \\ 0.2257849, & \text{sc lattice.}\end{cases}\end{aligned} \tag{53}$$

Equations (29) and (47) agree precisely with (52) to the order calculated, with the shape factor γ given by (53) for the sc lattice, and $\gamma = 0.1128924797$ for the bcc lattice (note that again γ for the bcc lattice is half that for the sc lattice), and with $\Sigma = M^+_\infty$ given in Eq. (28) and the spin-stiffness constant ρ_s given by

$$\rho_s = v^2\chi_\perp = \begin{cases} S^2[1 - 0.029778698/S - 0.00084(4)/S^2], & \text{sc lattice,} \\ S^2[1 - 0.0227993582/S - 0.00044(2)/S^2], & \text{bcc lattice.}\end{cases} \tag{54}$$

as may be verified by a direct calculation.[39]

Thus the spin-wave results are consistent in every detail with the predictions of effective-Lagrangian theory, as one should expect, and in addition they give explicit expressions for the parameters v, ρ_s, and Σ of the effective Lagrangian.

IV. SERIES ANALYSIS

The analysis of the series has been carried out along the same lines as in our previous papers[3,10] and we will not repeat the details here. First, we have endeavored, by use of Dlog Padé approximants, to test whether the

TABLE VI. Estimates of singularity parameters for the series given in Tables I – IV. Both unbiased estimates and estimates biased by setting $x_c^2 = 1$ are listed. The index values predicted by spin wave theory are also given for comparison.

Function	Singular point x_c^2	Singularity index unbiased	Singularity index biased	Spin-wave prediction
Spin-$\frac{1}{2}$ XXZ model on the sc lattice				
m	1.0(2)	0.6(3)	0.52(3)	0.5
$\frac{d\chi_\parallel^S}{dx^2}$	1.0(4)	−1.2(10)	−1.2(2)	−1.0
$\frac{d^2M^+}{d(x^2)^2}$	—	—	−1.1(5)	−1.0
$\frac{d^3E_0}{d(x^2)^3}$	—	—	—	−1.0
$\frac{d^2\chi_\perp}{dx^2}$	$x_c = 0.7(5)$	0.2(3)[a]	−0.8(6)	−1.0
$\chi_\perp^S$	$x_c = 1.002(1)$	−1.03(5)	−1.01(3)	−1.0
Spin-1 XXZ model on the sc lattice				
m	1.005(8)	0.52(5)	0.51(2)	0.5
$\frac{d\chi_\parallel^S}{dx^2}$	1.06(10)	−1.4(4)	−1.2(3)	−1.0
$\frac{d^2M^+}{d(x^2)^2}$	1.1(3)	−1.4(6)	−1.2(3)	−1.0
$\frac{d^3E_0}{d(x^2)^3}$	1.1(4)	−1.5(10)	−1.4(5)	−1.0
$\frac{d^2\chi_\perp}{dx^2}$	$x_c = 0.8(5)$	—	−2.6(2.0)	−1.0
$\chi_\perp^S$	$x_c = 1.001(2)$	−1.02(4)	−1.01(2)	−1.0
Spin-$\frac{1}{2}$ XXZ model on the bcc lattice				
m	1.01(5)	0.53(6)	0.51(3)	0.5
$\frac{d\chi_\parallel^S}{d(x^2)}$	1.02(10)	−1.4(5)	−1.2(3)	−1.0
$\frac{d^2M^+}{d(x^2)^2}$	1.08(10)	−1.5(6)	−1.2(3)	−1.0
$\frac{d^3E_0}{d(x^2)^3}$	1.0(3)	−1.5(10)	−1.4(6)	−1.0
$\frac{d^2\chi_\perp}{dx^2}$	$x_c = 0.7(5)$	0.2(4)[a]	−0.5(7)	−1.0
$\chi_\perp^S$	$x_c = 1.001(2)$	−1.02(3)	−1.01(2)	−1.0
Spin-1 XXZ model on the bcc lattice				
m	1.001(8)	0.51(4)	0.505(10)	0.5
$\frac{d\chi_\parallel^S}{d(x^2)}$	1.05(8)	−1.4(6)	−1.1(4)	−1.0
$\frac{d^2M^+}{d(x^2)^2}$	1.04(6)	−1.4(5)	−1.1(3)	−1.0
$\frac{d^3E_0}{d(x^2)^3}$	series too short	—	—	−1.0
$\frac{d^2\chi_\perp}{dx^2}$	$x_c = 0.7(5)$	0.03(10)[a]	−0.9(5)	−1.0
$\chi_\perp^S$	$x_c = 1.001(6)$	−1.01(4)	−1.007(10)	−1.0
Spin-$\frac{1}{2}$ XY model on the sc lattice				
$\frac{d^2M_z}{d(x^2)^2}$	1.03(6)	−1.3(5)	−1.2(3)	−1.0
$\frac{d^3E_0}{d(x^2)^3}$	1.1(4)	−1.7(6)	−1.4(4)	−1.0
$\frac{d\chi_{zz}}{d(x^2)}$	1.02(4)	−1.3(5)	−1.2(3)	−1.0
m $(x > 0)$	$x_c = 1.001(4)$	0.52(4)	0.51(2)	0.5
χ_{yy} $(x > 0)$	$x_c = 1.001(2)$	−1.01(3)	−1.007(10)	−1.0
$\frac{d^2\chi_{yy}}{dx^2}$ $(x < 0)$	$x_c = -0.9(3)$	−0.06(10)[a]	−0.9(5)	−1.0
$\frac{d^3\chi_{zz}}{dx^3}$ $(x > 0)$	$x_c = 1.0(8)$	−1.2(8)	−1.4(10)	−1.0
$\frac{d^3\chi_{zz}}{dx^3}$ $(x < 0)$	$x_c = -1.0(6)$	−0.8(8)	−0.9(4)	−1.0

TABLE VI. *(Continued)*.

Function	Singular point x_c^2	Singularity index unbiased	Singularity index biased	Spin-wave prediction
Spin-$\frac{1}{2}$ XY model on the bcc lattice				
$\frac{d^2 M_z}{d(x^2)^2}$	1.04(5)	−1.3(4)	−1.1(3)	−1.0
$\frac{d^3 E_0}{d(x^2)^3}$	1.1(3)	−1.6(5)	−1.3(4)	−1.0
$\frac{d\chi_{zz}}{d(x^2)}$	1.04(4)	−1.3(4)	−1.1(3)	−1.0
m $(x>0)$	$x_c = 1.001(3)$	0.51(2)	0.505(10)	0.5
χ_{yy} $(x>0)$	$x_c = 1.003(5)$	−1.03(4)	−1.008(10)	−1.0
$\frac{d^2\chi_{yy}}{dx^2}$ $(x<0)$	$x_c = -0.9(4)$	−0.04(10)[a]	−0.9(5)	−1.0
$\frac{d^3\chi_{zz}}{dx^3}$ $(x>0)$	$x_c = 1.0(4)$	−1.4(10)	−1.4(2)	−1.0
$\frac{d^3\chi_{zz}}{dx^3}$ $(x<0)$	$x_c = -0.8(4)$	−1.2(10)	−1.0(2)	−1.0
Spin-$\frac{1}{2}$ XY model on the fcc lattice				
$\frac{d^2 M_z}{dx^2}$	$x_c = 1.01(8)$	−1.2(6)	−1.2(3)	−1.0
$\frac{d^3 E_0}{dx^3}$	$x_c = 1.02(6)$	−1.3(5)	−1.2(3)	−1.0
$\frac{d\chi_{zz}}{dx}$	$x_c = 1.004(7)$	−1.08(10)	−1.06(5)	−1.0
m $(x>0)$	$x_c = 1.001(8)$	0.51(6)	0.507(10)	0.5
χ_{yy} $(x>0)$	$x_c = 1.0006(10)$	−1.01(2)	−1.008(10)	−1.0
$\frac{d^3\chi_{zz}}{dx^3}$ $(x>0)$	$x_c = 1.1(4)$	−1.4(4)	−1.4(2)	−1.0

[a] All estimates defective.

TABLE VII. Series estimates for the leading-order amplitudes A_n of the spin-$\frac{1}{2}$ and spin-1 Heisenberg antiferromagnets at $x = 1$ [as defined by Eq. (55) or Eq. (56) as the case may be]. Also listed are the spin-wave predictions at first, second, and third order.

Function	n	Amplitudes A_n Spin-wave predictions First order	Second order	Third order	Series estimate
Spin-$\frac{1}{2}$ XXZ model on the sc lattice					
E_0/N	0	−0.895737	−0.9028168	−0.902498(1)	−0.9021(2)
	2	0.190405	0.160566	0.1624(7)	0.1605(10)
M^+	0	0.421642	0.4216423	0.42272(1)	0.424(2)
	1	−0.065810	−0.032395	−0.040(1)	−0.0374(6)
$\chi_\perp$	0	1/12	0.0621772	0.0643772(1)	0.0653(5)
	1		−0.0219367	−0.0081(2)	−0.0100(2)
m	1	3	2.529854	2.527249(1)	2.56(4)
	2		−0.394860	−0.13(4)	−0.20(4)
$\chi_\parallel^S$	−1	−0.0438734	−0.0396107	−0.0381(3)	−0.03824(10)
	0	−0.028781	−0.0037081	−0.008(3)	−0.011(5)
$(1-x)\chi_\perp^S$	0	1/6	0.208979	0.2155(2)	0.2144(10)
	1		0.0438734	0.0331(4)	0.0314(4)
Spin-1 XXZ model on the sc lattice					
E_0/N	0	−3.29147	−3.2985538	−3.2983942(4)	−3.2977(8)
	2	0.380811	0.3509716	0.3519(3)	0.345(6)
M^+	0	0.921642	0.9216423	0.921912(2)	0.924(2)
	1	−0.065810	−0.049103	−0.0509(3)	−0.050(4)
$\chi_\perp$	0	1/12	0.0727553	0.07330528(2)	0.0737(5)
	1		−0.0109683	−0.00752(5)	−0.0072(10)
m	1	6	5.529854	5.5285514(6)	5.55(2)
	2		−0.394860	−0.26(2)	−0.26(4)
$\chi_\parallel^S$	−1	−0.0219367	−0.0208710	−0.02068(4)	−0.019(1)
	0	−0.0143905	−0.0081223	−0.0086(3)	−0.009(4)
$(1-x)\chi_\perp^S$	0	1/6	0.187823	0.18946(5)	0.1887(4)
	1		0.02193668	0.0192(1)	0.017(2)
Spin-$\frac{1}{2}$ XXZ model on the bcc lattice					
E_0/N	0	−1.146075	−1.151410	−1.1512341(2)	−1.1510(5)
	2	0.191674	0.168935	0.1701(1)	0.167(3)
M^+	0	0.4406818	0.4406818	0.441159(5)	0.442(4)
	1	−0.05066	−0.0312399	−0.0346(2)	−0.0333(10)
$\chi_\perp$	0	1/16	0.05052037	0.05144241(4)	0.0519(3)
	1		−0.012665148	−0.0069(2)	−0.012(2)
m	1	4	3.52545445	3.523949(4)	3.55(10)

TABLE VII. (*Continued*).

Function	n	Amplitudes A_n Spin-wave predictions First order	Second order	Third order	Series estimate
	2		−0.405284735	−0.217(8)	−0.24(4)
$\chi_{\parallel}^{S}$	−1	−0.0253303	−0.02348023	−0.0230(2)	−0.0224(6)
	0	−0.0172419	−0.00627227	−0.0076(5)	−0.006(2)
$(1-x)\chi_{\perp}^{S}$	0	1/8	0.148959257	0.15184(8)	0.15109(8)
	1		0.025330296	0.021(1)	0.018(4)
Spin-1 XXZ model on the bcc lattice					
E_0/N	0	−4.2921507	−4.297485	−4.2973975(2)	−4.2961(8)
	2	0.383348	0.360609	0.3612(1)	0.35(2)
M^+	0	0.9406818	0.9406818	0.940800(1)	0.942(3)
	1	−0.05066	−0.04095	−0.04178(5)	−0.042(2)
$\chi_{\perp}$	0	1/16	0.056510186	0.05674070(1)	0.0570(3)
	1		−0.006332574	−0.00488(5)	−0.056(8)
m	1	8	7.525454451	7.524702(2)	7.55(4)
	2		−0.405284735	−0.311(4)	−0.31(3)
$\chi_{\parallel}^{S}$	−1	−0.01266515	−0.01220263	−0.01214(3)	−0.0109(4)
	0	−0.00862095	−0.00587854	−0.00604(6)	−0.007(3)
$(1-x)\chi_{\perp}^{S}$	0	1/8	0.136979629	0.13770(2)	0.1372(6)
	1		0.012665148	0.0116(3)	0.01004(4)

TABLE VIII. Series estimates for the leading-order amplitudes A_n in an asymptotic expansion at $x=\pm1$ [defined by Eq. (55) or Eq. (56) as the case may be] of the spin-$\frac{1}{2}$ XY model on the simple cubic lattice. Also listed are the spin-wave predictions at first and second order (Ref. 30).

Function	x	n	Amplitudes A_n Spin-wave predictions First order	Second order	Series estimate
Spin-$\frac{1}{2}$ XY model on the sc lattice					
E_0/N	±1	0	−0.787898	−0.791402	−0.79177(16)
		2	0.052735	0.050532	0.0495(8)
M_x	±1	0	0.477476	0.476125	0.4765(5)
		1	−0.0232674	−0.0161322	−0.0166(4)
χ_{xx}	±1	−1	−0.0155116	−0.0136349	−0.0128(3)
		0	−0.014898	−0.007157	−0.007(2)
$(1-x)^{-1/2}m$	1	0	3	2.78864	2.81(2)
		1		−0.558416	−0.48(4)
$(1-x)^{-1/2}m$	−1	0	3	2.94107	2.860(6)
		2		0.172831	0.40(2)
$(1-x)\chi_{yy}$	1	0	1/6	0.190104	0.1912(10)
		1		0.0310232	0.022(4)
χ_{yy}	−1	0	1/12	0.0716145	0.0728(5)
		1		−0.0155116	−0.0084(12)
χ_{zz}	1	0	1/6	0.151697	0.15031(6)
		2		0.0192034	0.0180(3)
χ_{zz}	−1	0	1/6	0.181636	0.18548(4)
		2		−0.0192034	−0.0227(2)
Spin-$\frac{1}{2}$ XY model on the bcc lattice					
E_0/N	±1	0	−1.03801	−1.04064	−1.0408(2)
		2	0.0531571	0.0514454	0.0505(8)
M_x	±1	0	0.4829234	0.48216512	0.4824(5)
		1	−0.01791122	−0.01375463	−0.0139(1)
χ_{xx}	±1	−1	−0.0089556	−0.0081353	−0.0074(4)
		0	−0.00877273	−0.00539716	−0.0055(5)
$(1-x)^{-1/2}m$	1	0	4	3.7856355	3.808(10)
		1		−0.57315917	−0.36(2)
$(1-x)^{-1/2}m$	−1	0	4	3.94113886	3.888(4)
		2		0.17375268	0.32(2)
$(1-x)\chi_{yy}$	1	0	1/8	0.13828928	0.13872(10)
		1		0.01791122	0.0152(6)
χ_{yy}	−1	0	1/16	0.05585536	0.0563(2)
		1		−0.00895562	−0.006(1)
χ_{zz}	1	0	1/8	0.1165702	0.11600(6)
		2		0.01085954	0.0103(4)
χ_{zz}	−1	0	1/8	0.1334298	0.13493(2)
		2		−0.01085954	−0.0120(4)
Spin-$\frac{1}{2}$ XY model on the fcc lattice					
E_0/N	±1	0	−1.5440401	−1.54614316	−1.5462(2)
		2	0.1321351	0.12743321	0.125(3)
M_x	±1	0	0.4853175	0.48496947	0.4856(4)
		1	−0.032905	−0.02645997	−0.0256(10)
χ_{xx}	±1	−1	−0.0054842	−0.00505414	−0.0038(6)
		0	−0.0094250	−0.00747821	−0.006(2)
$(1-x)^{-1/2}m$	1	0	6	5.70568	5.73(6)
		1		−0.78972047	−0.51(3)
$(1-x)\chi_{yy}$	1	0	1/12	0.09067417	0.0908(2)
		1		0.01096834	0.0098(8)
χ_{zz}	1	0	1/12	0.07927384	0.07919(2)
		2		0.00570016	0.0052(2)

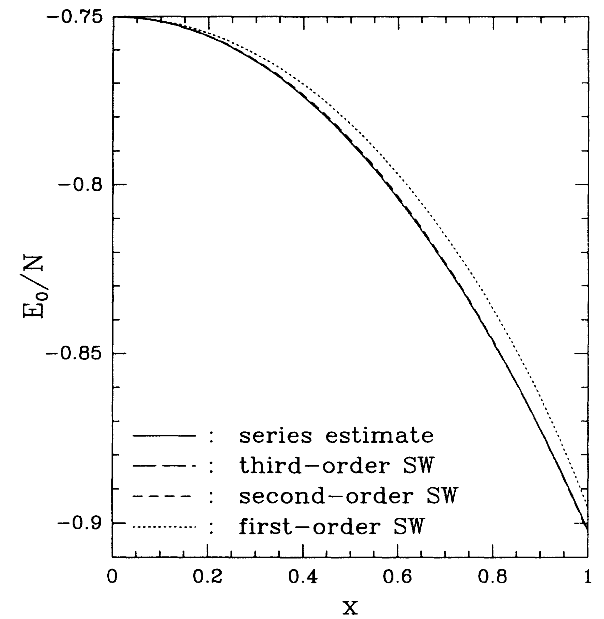

FIG. 2. Graph of the ground-state energy per site E_0/N against x for the spin-$\frac{1}{2}$ Heisenberg antiferromagnet on the sc lattice. The four curves shown are the series estimate, and the first-, second-, and third-order spin-wave predictions, corresponding to solid, dotted, short-dashed, and long-dashed lines, respectively.

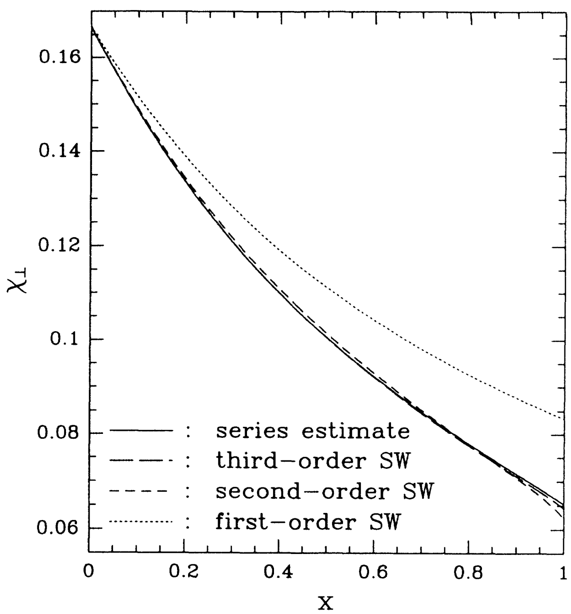

FIG. 4. Graph of the perpendicular susceptibility $\chi_\perp$ against x for spin-$\frac{1}{2}$ Heisenberg antiferromagnet on the sc lattice. Notation as Fig. 2.

singularities of these functions at $x = \pm 1$ are of the form predicted by spin-wave theory.[30] The results, given in Table V, show that the singularities and the indices are by and large quite consistent with the predictions of spin-wave theory. For the XXZ and XY models on the sc and bcc lattices, just as for the square lattice,[3,10] we did not get very consistent results between the series estimates and spin-wave theory for the singularity of the ground-state energy series, because the series is too short and the singularity is very weak. But for the XY ferromagnet on the fcc lattice, we have a longer series, and Table VI does show that the singularity of the ground-state energy is of the form predicted by spin-wave theory.

Next, we assume the singularities are those pre-

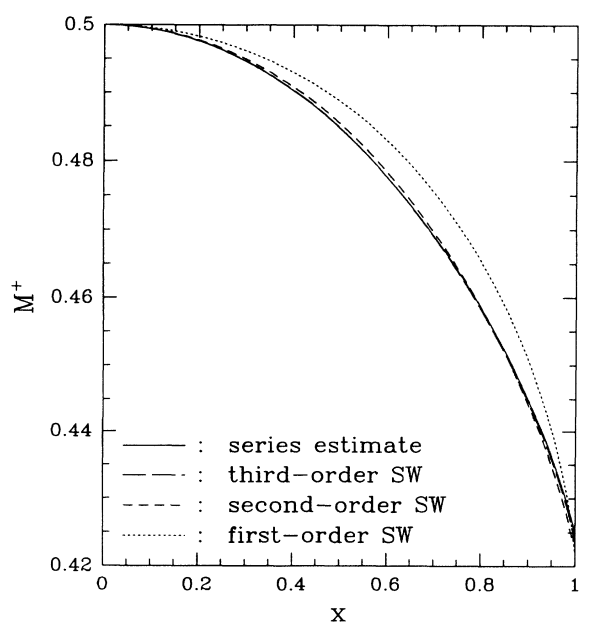

FIG. 3. Graph of the staggered magnetization M^+ against x for the spin-$\frac{1}{2}$ Heisenberg antiferromagnet on the sc lattice. Notation as Fig. 2.

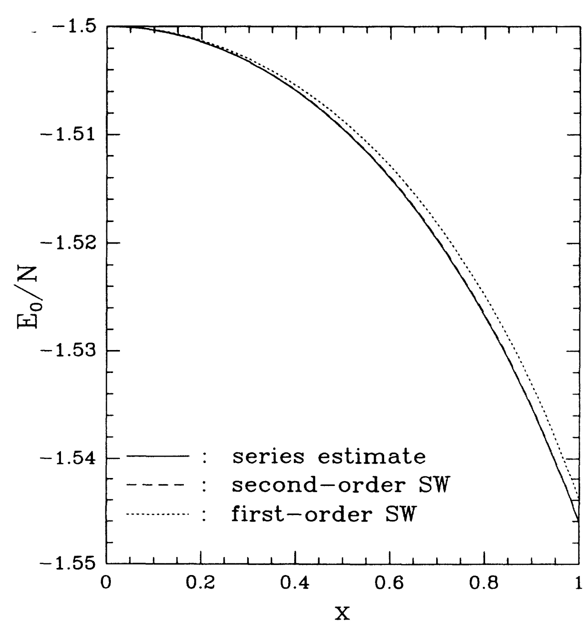

FIG. 5. Graph of the ground state energy per site E_0/N against x for the spin-$\frac{1}{2}$ XY ferromagnet on the fcc lattice. The three curves shown are the series estimate, and the first- and second-order spin-wave predictions, corresponding to solid, dotted and short-dashed lines, respectively.

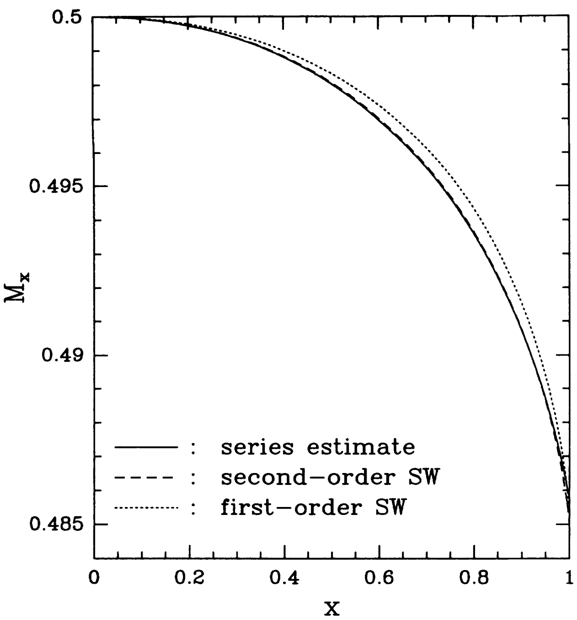

FIG. 6. Graph of the magnetization M_x against x for the spin-$\frac{1}{2}$ XY ferromagnet on the fcc lattice. Notation as Fig. 5.

dicted by spin-wave theory, and estimate, by using integrated differential approximants,[37] the coefficients of the leading-order terms for each given function $f(x)$ in the asymptotic expansion near $x = \pm 1$ defined by

$$f(x) = \sum_{n=n_0}^{\infty} A_n F_n(x) \qquad (x \sim 1) \tag{55}$$

or

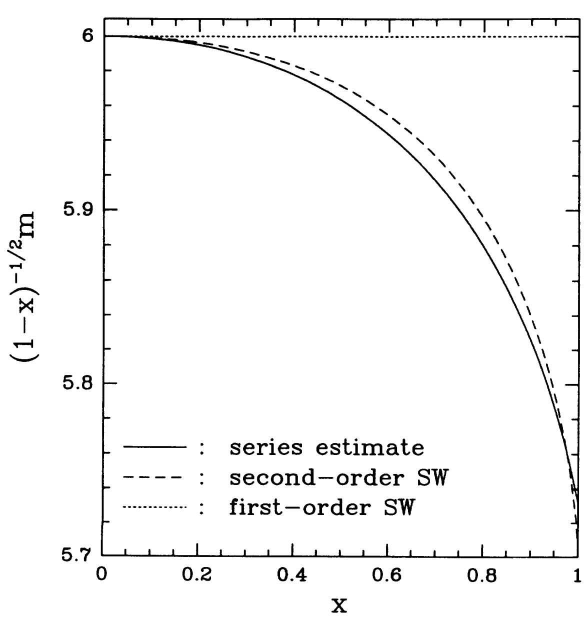

FIG. 7. Graph of the energy gap $(1-x)^{-1/2}m$ against x for the spin-$\frac{1}{2}$ XY ferromagnet on the fcc lattice. Notation as Fig. 5.

$$f(x^2) = \sum_{n=n_0}^{\infty} A_n F_n(x^2) \qquad (x \sim \pm 1), \tag{56}$$

where $F_{-1}(x) = \ln(1-x)$, $F_0 = 1$, $F_1(x) = (1-x)\ln(1-x)$, and $F_2(x) = (1-x)$. Our series estimates of these amplitudes A_n are listed in Tables VII and VIII, together with the predictions of spin-wave theory at first, second, and third order in $1/S$.

The agreement between the spin-wave predictions and the series estimates is very good. The leading-order amplitudes obtained from the two approaches agree within errors in 50% of cases, and even where they disagree, the proportional discrepancy is very small. The confidence level thus obtained for the ground-state energy is of order 0.05%, and for the other quantities it is mostly of order 0.5%. The agreement is further illustrated in Figs. 2–7 which graph the series estimates and spin-wave predictions as functions of x for E_0/N, M^+, and $\chi_\perp$ for the spin-$\frac{1}{2}$ Heisenberg on the sc lattice, and for the XY ferromagnet on the fcc lattice. The higher-order spin-wave results are barely, if at all, distinguished from the series estimates on these plots.

Making comparison with earlier work, we find that Nishimori and Miyake[21] have previously obtained second-order spin-wave estimates of the ground-state energy for both models in precise agreement with ours. The series approach of Parrinello and Arai[26] gave results for the Heisenberg model which were within 0.2% of ours for the ground-state energy and 2% for the magnetization. The finite-cell estimates of Oitmaa and Betts[29] give similar results for the ground-state energy, within errors of order 10%, but appear to underestimate the staggered magnetization. A comparison of these various results is given in Table IX. Note that we have arbitrarily assigned an error to our spin-wave estimates equal to one-half the difference between the second-order and third-order results.

V. SUMMARY AND CONCLUSIONS

A number of properties of the Heisenberg antiferromagnet and the XY model have been calculated for three-dimensional lattices, using both series expansions about the Ising limit and spin-wave theory. The accuracy of the series results at the isotropic point is typically within 0.05% for the ground-state energy, and about 0.5% for other quantities. The results of the two different methods are generally consistent to within this same level of accuracy, giving us confidence in the power and accuracy of them both.

It has been known since the early days[17–20] that spin-wave theory gives a good description of the Heisenberg antiferromagnet. The disordering effect of quantum fluctuations is generally smaller in three dimensions than in two, and spin-wave theory leads to an expansion in powers of $(zS)^{-1}$, where z is the coordination number, which is generally larger in three dimensions than in two. This conclusion is further reinforced by our results. At the isotropic point, first-order spin-wave theory differs from

TABLE IX. A comparison of the present estimates of ground-state energy and magnetization with previous estimates for the $S = \frac{1}{2}$ Heisenberg antiferromagnet.

Reference	Method	sc lattice		bcc lattice	
		$-E_0/N$	M^+	$-E_0/N$	M^+
Nishimori and Miyake[a]	spin wave	0.9028	–	1.1515	–
Parrinello and Arai[b]	series	0.9010	0.4321	1.1495	0.4494
Oitmaa and Betts[c]	finite cell	0.85(10)	0.30(2)	1.1(1)	0.31(2)
Present work	spin wave	0.9025(2)	0.4227(5)	1.1512(1)	0.4412(3)
Present work	series	0.9021(2)	0.424(2)	1.1510(5)	0.442(4)

[a]Reference 21.
[b]Reference 26.
[c]Reference 29.

the series results by about 1% for the ground-state energy and magnetization, and by amounts of order 20% for other quantities. Second-order spin-wave theory is an order of magnitude more accurate. Third-order spin-wave theory continues to converge, and is indistinguishable from the series results, within errors. In fact, the small changes between second and third order indicate that third-order spin-wave theory is *more* accurate, quantitatively, than the series results, although it is hard to give objective estimates of the errors. This is the reverse of the situation in two dimensions.[3,5]

The finite-size scaling corrections resulting from spin-wave theory have also been obtained for the isotropic Heisenberg antiferromagnet, and compared with the predictions of effective-Lagrangian theory. The two approaches turn out to be perfectly consistent, as one should expect, since they are both based on the effects of massless spin-wave excitations.

Theoretical estimates of high accuracy have thus been obtained for various measurable quantities in these models. We hope to make some numerical comparisons with experimental work on suitable systems[11] such as $CuCl_2{\cdot}2H_2O$, $KNiF_3$, or $RbMnF_3$ in the future.

ACKNOWLEDGMENT

This work forms part of a research project supported by a grant from the Australian Research Council.

* Electronic-mail address: otja@newt.phys.unsw.edu.au
† Electronic-mail address: c.hamer@unsw.edu.au
‡ Electronic-mail address: w.zheng@unsw.edu.au

[1] For recent reviews, see T. Barnes, Int. J. Mod. Phys. C **2**, 659 (1991); E. Manousakis, Rev. Mod. Phys. **63**, 1 (1991).
[2] R.R.P. Singh, Phys. Rev. B **39**, 9760 (1989); **41**, 4873 (1990).
[3] W.H. Zheng, J. Oitmaa, and C.J. Hamer, Phys. Rev. B **43**, 8321 (1991).
[4] K.J. Runge, Phys. Rev. B **45**, 7229 (1992).
[5] C.J. Hamer, W.H. Zheng, and Peter Arndt, Phys. Rev. B **46**, 6276 (1992).
[6] W.H. Zheng and C.J. Hamer, Phys. Rev. B **47**, 7961 (1993).
[7] H. Neuberger and T. Ziman, Phys. Rev. B **39**, 2608 (1989).
[8] D.S. Fisher, Phys. Rev. B **39**, 11783 (1989).
[9] P. Hasenfratz and F. Niedermayer (unpublished).
[10] C.J. Hamer, J. Oitmaa, and W.H. Zheng, Phys. Rev. B **43**, 10789 (1991).
[11] L.J. de Jongh and A.R. Miedema, Adv. Phys. **23**, 1 (1974).
[12] D.D. Betts, in *Phase Transitions and Critical Phenomena*, edited by C. Domb and M.S. Green (Academic, New York, 1974), Vol. 3.
[13] D.C. Mattis, *The Theory of Magnetism I* (Springer-Verlag, New York, 1981).
[14] F.J. Dyson, E.N. Lieb, and B. Simon, J. Stat. Phys. **18**, 335 (1978).
[15] T. Kennedy, E.N. Lieb, and B.S. Shastry, Phys. Rev. Lett. **61**, 2582 (1988).
[16] K. Kubo and T. Kishi, Phys. Rev. Lett. **61**, 2585 (1988).
[17] P.W. Anderson, Phys. Rev. **86**, 694 (1952).
[18] R. Kubo, Phys. Rev. **87**, 568 (1952).
[19] T. Oguchi, Phys. Rev. **117**, 117 (1960).
[20] R.B. Stinchcombe, J. Phys. C **4**, L79 (1971).
[21] H. Nishimori and S. Miyake, Prog. Theor. Phys. Jpn. **73**, 18 (1985).
[22] G. Gomez-Santos and J.D. Joannopoulos, Phys. Rev. B **36**, 8707 (1987).
[23] W. Marshall, Proc. R. Soc. London A **232**, 48 (1955).
[24] H. Taketa and T. Nakamura, J. Phys. Soc. Jpn. **11**, 919 (1956).
[25] H.L. Davis, Phys. Rev. **120**, 789 (1960).
[26] M. Parrinello and T. Arai, Phys. Rev. B **10**, 265 (1974).
[27] K.W. Becker, H. Won, and P. Fulde, Z. Phys. B **75**, 335 (1989).
[28] M. Kim and J. Hong, Phys. Rev. B **44**, 6803 (1991).
[29] J. Oitmaa and D.D. Betts, Phys. Lett. **68A**, 450 (1978).
[30] W.H. Zheng, J. Oitmaa, and C.J. Hamer, Phys. Rev. B**44**, 11869 (1991).
[31] B.G. Nickel (unpublished).
[32] H.X. He, C.J. Hamer, and J. Oitmaa, J. Phys. A **23**, 1775 (1990).
[33] M.F. Sykes and M.K. Wilkinson, J. Phys. A **19**, 3407 (1986).
[34] M.F. Sykes, J. Phys. A **19**, 1007 (1986).

[35] M.F. Sykes, J.W. Essam, and D.S. Gaunt, J. Math. Phys. **6**, 283 (1965).
[36] M.F. Sykes, D.S. Gaunt, J.W. Essam, B.R. Heap, C.J. Elliott, and S.R. Mattingly, J. Phys. A **6**, 1498 (1973).
[37] A.J. Guttmann, in *Phase Transitions and Critical Phenomena*, edited by C. Domb and J. Lebowitz (Academic, New York, 1989), Vol. 13.
[38] P. Hasenfratz and H. Leutwyler, Nucl. Phys. B**343**, 241 (1990).
[39] C.J. Hamer, J. Oitmaa, and W.H. Zheng (unpublished).